



ELSEVIER

Contents lists available at ScienceDirect

Journal of Luminescence

journal homepage: [www.elsevier.com/locate/jlumin](http://www.elsevier.com/locate/jlumin)

## Newly synthesized benzanthrone derivatives as prospective fluorescent membrane probes



Olga Zhytniakivska<sup>a,\*</sup>, Valeriya Trusova<sup>a</sup>, Galyna Gorbenko<sup>a</sup>, Elena Kirilova<sup>b</sup>,  
Inta Kalnina<sup>b</sup>, Georgiy Kirilov<sup>b</sup>, Paavo Kinnunen<sup>c</sup>

<sup>a</sup> Department of Nuclear and Medical Physics, V.N. Karazin Kharkiv National University, 4 Svobody Square, Kharkiv 61077, Ukraine

<sup>b</sup> Department of Chemistry and Geography, Faculty of Natural Science and Mathematics, Daugavpils University, 13 Vienibas, Daugavpils LV5401, Latvia

<sup>c</sup> Department of Biomedical Engineering and Computational Science, School of Science and Technology, Aalto University, FI-00076 Espoo, Finland

### ARTICLE INFO

#### Article history:

Received 27 May 2013

Received in revised form

4 October 2013

Accepted 5 October 2013

Available online 12 October 2013

#### Keywords:

Fluorescence

Benzanthrone derivatives

Lipid membranes

Partitioning

### ABSTRACT

Fluorescence spectral properties of a series of novel benzanthrone derivatives have been explored in lipid bilayers composed of zwitterionic lipid phosphatidylcholine (PC) and its mixtures with cholesterol (Chol) and anionic phospholipid cardiolipin (CL). Analysis of partition coefficients showed that all the examined compounds possess rather high lipid-associating ability, with the amidino derivatives exhibiting stronger membrane partitioning compared with the aminobenzanthrones. To understand how benzanthrone partition properties correlate with their structure, quantitative structure property relationship (QSPR) analysis was performed involving a range of quantum chemical molecular descriptors.

© 2013 Elsevier B.V. All rights reserved.

### 1. Introduction

Among a wide variety of fluorescent dyes currently used in biomedical research and industry, benzanthrone derivatives attract particular interest due to their favorable spectral properties, viz. large extinction coefficient, marked Stokes shift, negligible fluorescence in an aqueous phase, high sensitivity of fluorescence parameters to environmental polarity, etc. [1,2]. Bright color and intense fluorescence of benzanthrone derivatives gave the impetus to their use as disperse dyes for textiles, polymers, daylight fluorescent pigments and lasers [3,4]. It has been demonstrated that some 3-oxy- and 3-azomethine substituted benzanthrone derivatives, of yellow-green or orange-red color, exhibit features which qualify them as appropriate components of liquid-crystal (LC) systems for electro-optic displays of the “guest–host” type [5,6]. The absorption properties of 3-substituted benzanthrone dyes are determined by the charge transfer within chromophoric system, occurring between electron-donating groups in the C-3 position and electron-accepting carbonyl group [7,8]. It is known that spectral behavior of the dyes emitting from an intramolecular charge transfer (ICT) state is highly sensitive to the surrounding environment (polarity, viscosity, formation of

hydrogen bonds or other intermolecular interactions) [9]. For this reason, ICT dyes represent effective microenvironmental sensors for monitoring structural changes in biological systems. In particular, benzanthrone derivatives were employed in DNA [10], protein [11] and membrane studies [12]. Furthermore, these dyes displayed pronounced sensitivity to the changes in immune status of a human organism at different pathologies [13,14].

Our recent study revealed high lipid-associating ability of a series of newly synthesized benzanthrone amino derivatives [12]. Moreover, spectral responses of the two examined dyes in different lipid systems proved to correlate with increased bilayer hydration. These findings allowed us to conclude that benzanthrone amino derivatives may be effective fluorescent probes for examining membrane-related processes, especially those coupled with the change in the degree of lipid bilayer hydration. In view of this it seemed of interest to extend our previous investigation to a new series of benzanthrone dyes (referred here as AM12, AM15, AM18, IAH, IBH and ISH), whose structures are given in Fig. 1. Our goal was three fold: (i) to obtain quantitative information about the dye partitioning into lipid phase of the model membranes composed of zwitterionic lipid phosphatidylcholine (PC) and its mixtures with cholesterol (Chol) and anionic phospholipid cardiolipin (CL); (ii) to assess benzanthrone sensitivity to the changes in physicochemical properties of lipid bilayer and (iii) to ascertain how benzanthrone partition behavior correlate with their structure and physicochemical properties via quantitative structure property relationship analysis (QSPR).

\* Correspondence to: 52–52 Tobolskaya Street, Kharkiv 61072, Ukraine.

Tel.: +380 57 3438244; fax: +380 57 7544746.

E-mail address: [olya\\_zhitniakivska@yahoo.com](mailto:olya_zhitniakivska@yahoo.com) (O. Zhytniakivska).

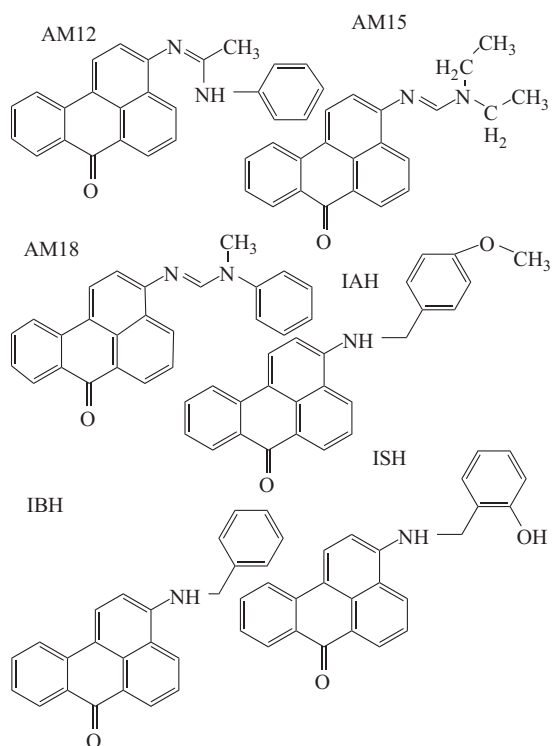


Fig. 1. Chemical structures of the examined benzanthrone dyes.

## 2. Materials and methods

### 2.1. Materials

Egg yolk phosphatidylcholine and beef heart cardiolipin were purchased from Biolek (Kharkov, Ukraine). Both phospholipids gave single spots by thin layer chromatography in the solvent system chloroform:methanol:acetic acid:water, 25:15:4:2, v/v. Chol was from Sigma. Benzanthrone dyes AM12, AM15, AM18, IAH, IBH and ISH were synthesized at the Faculty of Natural Sciences and Mathematics of Daugavpils University as described in detail elsewhere [15]. All other chemicals were of analytical grade and used without further purification.

### 2.2. Preparation of lipid vesicles

Unilamellar lipid vesicles composed of PC and its mixtures with (a) 5 or 10 mol% of CL or (b) 30 mol% of Chol were prepared by the extrusion method [16]. Thin lipid films were obtained by evaporation of lipids' ethanol solutions and then hydrated with 1.2 ml of 5 mM Na-phosphate buffer (pH 7.4). Lipid suspension was extruded through a 100 nm pore size polycarbonate filter. Phospholipid concentration was determined according to the procedure of Bartlett [17]. The dye-liposome mixtures were prepared by adding the proper amounts of the probe stock solutions in ethanol to liposome suspension.

### 2.3. Fluorescence measurements

Steady-state fluorescence spectra were recorded with an LS-55 spectrofluorimeter (Perkin-Elmer Ltd., Beaconsfield, UK) at 20 °C using 10 mm path-length quartz cuvettes. Excitation wavelengths were 470 nm for AM12, 480 nm for AM15, 460 nm for AM18 and 520 nm for IAH, IBH and ISH. Excitation and emission slit widths were set at 10 nm. Fluorescence quantum yields were measured

using rhodamine 101 as a standard. Absorption measurements were performed using an SF-46 spectrophotometer.

### 2.4. Calculations

Complete geometry optimization of the isolated molecules in the ground state was carried out using the semiempirical PM6 method. Quantum chemical calculations were performed with MOPAC 2012 Version10.006W-free academic license [18]. The energy of highest occupied molecular orbital ( $E_{HOMO}$ ), the energy of lowest unoccupied molecular orbital ( $E_{LUMO}$ ), cosmo area ( $cosAr$ ), cosmo volume (molecular volume) ( $cosVol$ ) and molecular length ( $L$ ), the charge on nitrogen atom at the C-3 position  $q(N)$  and the total charge on carbon atoms  $\sum q(C)$  were extracted directly from the data files following the geometry optimization. The dipole moments of the ground ( $\mu$ ) and excited ( $\mu_e$ ) states were calculated using ab-initio method at B3LYP/6-31G level of theory with GAMESS 11.

Virtual Computational Chemistry Laboratory (<http://www.vcclab.org>) was used for calculation of lipophilicity of the examined compounds.

## 3. Theory

Total concentration of the dye distributing between the aqueous and lipid phases ( $Z_{tot}$ ) can be represented as

$$Z_{tot} = Z_F + Z_L \quad (1)$$

where subscripts  $F$  and  $L$  denote free and lipid-bound dye, respectively. The coefficient of dye partitioning between two phases ( $K_p$ ) is defined as [19]

$$K_p = \frac{Z_L V_W}{Z_F V_L} \quad (2)$$

here  $V_W$  and  $V_L$  are the volumes of aqueous and lipid phases, respectively. Given that under the employed experimental conditions the volume of the lipid phase is much less than the total volume of the system  $V_t$ , we assume that  $V_W \approx V_t = 1 \text{ dm}^3$ . It is easy to show that

$$Z_F = \frac{Z_{tot} V_W}{V_W + K_p V_L} = \frac{Z_{tot}}{1 + K_p V_L} \quad (3)$$

The dye fluorescence intensity measured at a certain lipid concentration can be written as

$$I = a_f Z_F + a_l Z_L = Z_F \left( a_f + a_l \frac{K_p V_L}{V_W} \right) = Z_F (a_f + a_l K_p V_L) \quad (4)$$

where  $a_f$  and  $a_l$  represent molar fluorescence of the dye free in solution and in the lipid environment, respectively. From Eqs. (3) and (4) one obtains

$$I = \frac{Z_{tot} (a_f + a_l K_p V_L)}{1 + K_p V_L} \quad (5)$$

The volume of the lipid phase can be determined from

$$V_L = N_A C_L \sum v_i f_i \quad (6)$$

where  $C_L$  is the molar lipid concentration,  $f_i$  is mole fraction of the  $i$ th bilayer constituent,  $v_i$  is its molecular volume taken as  $1.58 \text{ nm}^3$ ,  $3 \text{ nm}^3$  and  $0.74 \text{ nm}^3$  for PC, CL and Chol respectively [20]. For Chol-containing systems condensing effects of this lipid was taken into account, so that the above  $v$  value for PC was reduced by the factor 1.3.

The relationship between  $K_p$  and fluorescence intensity increase ( $\Delta I$ ) upon the dye transfer from water to the lipid phase

can be written as [19]

$$\Delta I = I_L - I_W = \frac{K_p V_L (I_{max} - I_W)}{1 + K_p V_L} \quad (7)$$

where  $I_L$  is the fluorescence intensity observed in the liposome suspension at a certain lipid concentration  $C_L$ ,  $I_W$  is the dye fluorescence intensity in a buffer,  $I_{max}$  is the limit fluorescence in the lipid environment.

In terms of modern theories of the membrane electrostatics partition coefficient can be represented as consisting of electrostatic and nonelectrostatic terms [21,22]

$$K_p = \exp(\{w_{el} + w_{Born} + w_n + w_d\}/kT) \quad (8)$$

The first term  $w_{el}$  characterizes the Coulombic ion-membrane interactions

$$w_{el} = ze\psi_{el} \quad (9)$$

where  $ze$  is the dye charge;  $\psi_{el}$  is the membrane Coulomb potential. The contribution  $w_{Born}$  corresponds to free energy of charge transfer between the media with different dielectric constants;  $w_n$  is neutral energy term determined by hydrophobic, van der Waals and steric factors [23]. Of special interest is hydration contribution  $w_h$  related to the ability of membrane constituents to bind water molecules [22,24]. The term  $w_d$  depends on membrane dipole potential ( $\psi_d$ ). In general, membrane surface potential can be represented as a sum of common Coulomb dipole potential ( $\psi_{el}$ ) and non-Coulomb dipole potential ( $\psi_d$ ) originating from the molecular dipoles of phospholipids and interfacial water [21]. According to available estimates,  $\psi_d$  of model membranes has the magnitude of several hundred millivolts, being positive inside [23].

## 4. Results and discussion

### 4.1. The photophysical properties of benzanthrone derivatives

As indicated above, the photophysical properties of benzanthrone dyes strongly depend on electron donor–acceptor interaction within chromophoric system [8]. The occurrence of ICT state is controlled by electron-donating and electron-accepting powers of the fluorophore functional groups. The dyes under study are asymmetrical the amidino- and amino-benzanthrone derivatives of orange-red (AM12, AM15 and AM18) and crimson (IAH, IBH and ISH) color. These dyes were found to be nearly non-emissive in buffer but exhibited strong fluorescence in ethanol solution (Fig. 2). Presented in Table 1 are basic photophysical characteristics of the examined benzantrones in ethanol: absorption maximum ( $\lambda_A$ ), extinction

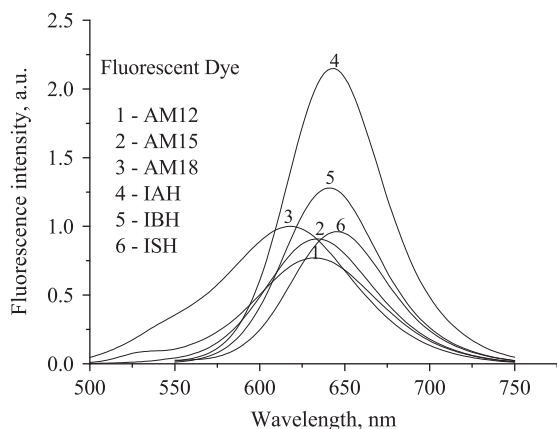


Fig. 2. Fluorescence spectra of benzanthrone derivatives in ethanol solution. Dye concentration was 2.1  $\mu\text{M}$  (a), 2.5  $\mu\text{M}$  (b), 1.9  $\mu\text{M}$  (c), 4.2  $\mu\text{M}$  (d), 3.1  $\mu\text{M}$  (e) and 2.8  $\mu\text{M}$  (f) for AM12, AM15, AM18, IAH, IBH and ISH, respectively.

Table 1

The basic photophysical characteristics of benzanthrone dyes in ethanol solution.

Parameter	AM12	AM15	AM18	IAH	IBH	ISH
$\lambda_A$ (nm)	469	475	465	524	531	529
$\lambda_F$ (nm)	628	632	618	644	642	644
$\log \epsilon$	3.85	4.15	3.53	3.60	3.80	2.82
$(\nu_A - \nu_F)$ ( $\text{cm}^{-1}$ )	5398	5229	5324	3556	3256	3375

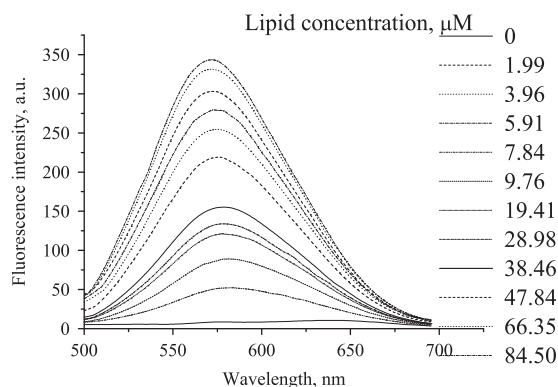


Fig. 3. Typical emission spectra of the amidino derivatives in PC lipid bilayer. AM15 concentration was 1.9  $\mu\text{M}$ .

coefficient ( $\epsilon$ ), emission maximum ( $\lambda_F$ ) and Stokes shift ( $\nu_A - \nu_F$ ). The higher  $\lambda_A$  values observed for ISH, IAH and IBH can be attributed to strong electron-donating power of amino group present in their structure [4]. The Stokes shifts were found to lie between 3000 and 5100  $\text{cm}^{-1}$ , falling in the range typical for this class of dyes [5]. As seen in Table 1 and Fig. 2,  $\lambda_A$  and  $\lambda_F$  of the amidinobenzantrones are hypsochromically shifted relative to the absorption and fluorescence maxima of the aminobenzantrones. As the photophysical properties of benzanthrone dyes strongly depend on the electron donor–acceptor interaction within the chromophoric system, the observed difference in maximum positions between AM12, AM15, AM18 and IAH, IBH, ISH is most likely associated with the higher electron-donating ability of amino group compared to that of amidino group [5]. Moreover, it should be noted that fluorescence maximum of IAH and ISH are red-shifted by 2 nm compared with IBH due to the presence of methoxy and hydroxy groups (electron donor) in their structure. It is also noteworthy that emission maximum of AM18 is hypsochromically shifted by 10 nm with regard to AM12 and by 14 nm compared with AM15. This, most probably, is connected with rotation of AM18 functional groups around the 3-(C–N) bond along with intramolecular charge redistribution upon electronic excitation. However, one cannot rule out the possibility that amino substitution of AM18 is more shifted out from the benzanthrone plane, in contrast to AM12 and AM15, thereby substantially affecting charge redistribution in amino group [15].

### 4.2. Binding studies

At the first step of the study we compared the lipophilic properties of benzanthrone dyes and their sensitivity to the changes in membrane environment. Emission spectra of these dyes were recorded in buffer solution (5 mM Na-phosphate, pH 7.4) and liposomal suspensions. Typical fluorescence spectra measured at increasing lipid concentration are presented in Fig. 3. Fluorescence intensity and quantum yield were found to increase upon the dye transfer from aqueous to lipid phase (Table 2), with emission maximum being shifted to lower wavelengths. The observed fluorescence enhancement is most likely to arise from

**Table 2**  
Partition coefficients and quantum yields of benzanthrone dyes in different systems.

Dye	System	Quantum yield	Partition coefficient, $K_p \times 10^4$
AM12	Buffer	0.02	
	PC	0.6	$18 \pm 0.8$
	PC/CL (5%)	0.5	$8.7 \pm 0.3$
	PC/CL (10%)	0.3	$5.8 \pm 0.6$
	PC/Chol (30%)	0.24	$15 \pm 1.5$
AM15	Buffer	0.02	
	PC	0.6	$6.1 \pm 0.2$
	PC/CL (5%)	0.47	$2.7 \pm 0.2$
	PC/CL (10%)	0.36	$1.6 \pm 0.5$
	PC/Chol (30%)	0.3	$4.9 \pm 0.4$
AM18	Buffer	0.05	
	PC	0.7	$12 \pm 0.8$
	PC/CL (5%)	0.4	$9.7 \pm 0.6$
	PC/CL (10%)	0.2	$7.7 \pm 0.5$
	PC/Chol (30%)	0.5	$7.8 \pm 0.5$
IAH	Buffer	0.004	
	PC	0.06	$4.8 \pm 0.5$
	PC/CL (5%)	0.05	$7.6 \pm 0.5$
	PC/CL (10%)	0.04	$5.4 \pm 0.1$
	PC/Chol (30%)	0.04	$6.8 \pm 0.8$
IBH	Buffer	0.003	
	PC	0.13	$6.0 \pm 0.4$
	PC/CL (5%)	0.06	$11 \pm 0.6$
	PC/CL (10%)	0.03	$11 \pm 0.1$
	PC/Chol (30%)	0.02	$9.8 \pm 0.7$
ISH	Buffer	0.003	
	PC	0.09	$6.1 \pm 0.5$
	PC/CL (5%)	0.08	$8.8 \pm 0.4$
	PC/CL (10%)	0.07	$7.0 \pm 0.4$
	PC/Chol (30%)	0.1	$6.2 \pm 0.2$

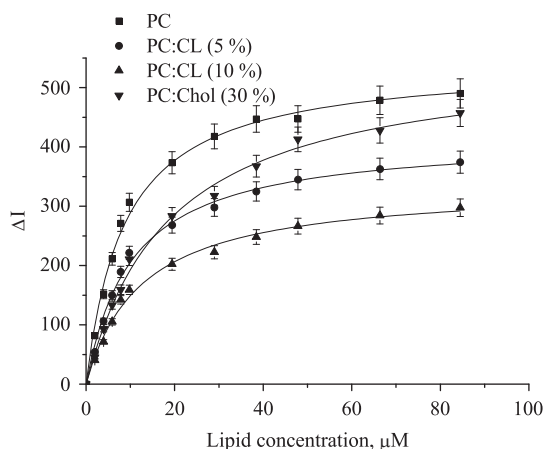


**Fig. 4.** The typical isotherms of benzanthrone binding to model membranes. AM18 concentration was  $2.3 \mu\text{M}$ .

reduced polarity of the dye lipid surroundings and restricted fluorophore mobility within lipid bilayer.

Next, it was of interest to ascertain how the dye lipid-associating ability depends on the membrane physical properties being varied through introducing anionic phospholipid (CL) or sterol (Chol) into the PC bilayer. Fluorescence spectroscopy technique was employed to quantify the dye partitioning into the lipid phase. To derive the dye partition coefficients in different lipid systems, experimental dependencies  $\Delta I(C_L)$  (Fig. 4) were approximated by Eq. (7). The resulting binding curves were hyperbolic in shape for all dyes under study except of the amidinobenzanthrone

derivative IAH for which experimental dependencies  $\Delta I(C_L)$  were linear. This means that the titration of benzanthrone AM12, AM15, AM18, IBH and ISH by liposomes was accompanied by saturation of partitioning curves at a lipid concentration  $\sim 85 \mu\text{M}$  (see Supplementary materials). The fluorescent dye IAH seems to be less prone to association with lipid vesicles, as the plateau is not reached even at a lipid concentration of  $100 \mu\text{M}$ . As seen in Table 2, addition of CL and Chol to PC bilayer gives rise to an increase in partition coefficients for IBH, ISH and IAH (relative to the neat PC membrane), whereas AM12, AM15 and AM18 exhibit the opposite behavior. Since spectral properties of benzanthrone dyes strongly depend on the nature of fluorophore environment, such as polarity, viscosity, the probability of hydrogen bonding and other intermolecular interactions, to interpret the observed differences in the  $K_p$  values, the influence of Chol and CL on the lipid bilayer structure should be considered. In liquid-crystalline lipid phase cholesterol can produce: (i) an increase in separation of phospholipid headgroups [25]; (ii) increased freedom of motion of the phosphocholine moiety [26]; (iii) enhanced headgroup hydration [27]; (iv) reduced content of acyl chain gauche conformation [28]; (v) tighter lateral packing of lipid molecules due to condensing effects [29] and (vi) higher dipole potential of the lipid bilayer [30]. MD simulation showed that interactions of Chol with PC and water at the membrane/water interface involve the formation of hydrogen bonds between Chol hydroxyl group and oxygen atoms of phosphate, carbonyl or water [31]. Later studies revealed that in the simulated PC–Chol membrane the number of water molecules hydrogen-bonded to PC headgroups is greater than that in the neat PC membrane [32], indicating larger water content in Chol-containing bilayers. The changes in the lipid packing density in the presence of Chol cause more water molecules to penetrate into the bilayer interior [31]. It is likely that Chol-induced packing defects facilitate bilayer incorporation of IBH, ISH and IAH, resulting in the increase in the partition coefficient compared to the neat PC membrane. It has also been reported that CL has the ability to change bilayer hydration. Specifically, according to Shibata et al., significant decrease in water permeability of the PC bilayer occurs on incorporation of small amounts of CL [33]. On the basis of FTIR data, they hypothesized that CL is capable of enhancing the hydration of ester's C=O groups and inducing a cooperative conformational change in the PC head groups [33]. These changes were assumed to involve displacement of the  $\text{N}^+$  end of P–N dipole toward orientation more parallel to the membrane surface, thereby resulting in rearrangement of water bridges at the bilayer surface and stabilization of the intermolecular hydrogen-bonded network including hydration water. The stability of this network was found to be influenced by the charged moiety of cardiolipin and the ester's carbonyl group [34]. It is noted that the change in hydration extent may considerably affect molecular organization of a lipid bilayer. In particular, increase in water content in the headgroup membrane region alters the alignment of the choline–phosphate dipole and lateral packing of the hydrocarbon region [35].

The relative contribution of the above factors seems to be different for the amino- and amidino-benzanthrone derivatives. Therefore, it seems of importance to discuss possible localization of these dyes in the model membranes. Since the ground state dipole moments of benzanthrone dyes are rather high (see Table 3), at first glance it seems energetically unfavorable for probes to penetrate into the hydrophobic membrane region, and they most probably reside in the membrane's polar part. Moreover, since a carbonyl group and a polar hydroxyl group (IAH) are present in the dye structure, they tend to form intermolecular hydrogen bonds with water and polar groups of lipids, suggesting their localization in the polar region of the lipid bilayer. However, given that the partition coefficients of AM12, AM15 and AM18

**Table 3**  
Quantum chemical characteristics of amidino- and aminobenzanthrones.

	Log $P_{o/w}$	$\mu$ (D)	$\mu_e$ (D)	$E_{HOMO}$ (eV)	$E_{LUMO}$ (eV)	$\cos Ar$ ( $\text{\AA}^2$ )	$\cos Vol$ ( $\text{\AA}^3$ )	$L$ (Å)	$\sum q(C)$ (C)	$q(N)$ (C)
AM12	7.18	6.05	12.56	−8.33	−1.21	377.4	426.7	17.3	−1.35	−0.54
AM15	5.54	5.72	10.9	−8.36	−1.19	355.0	400.1	14.6	−1.76	−0.46
AM18	6.57	6.11	11.89	−8.26	−1.30	374.3	443.2	15.1	−1.54	−0.48
ISH	5.28	4.36	11.82	−8.62	−1.44	358.1	406.1	14.9	−1.78	−0.41
IBH	5.76	3.61	10.41	−8.45	−1.27	351.8	395.6	14.94	−1.79	−0.42
IAH	5.85	4.12	11.13	−8.34	−1.30	381.0	427.6	14.95	−1.34	−0.45

**Table 4**  
Correlation matrix for physicochemical descriptors of AM12, AM15 and AM18.

	Log $P_{o/w}$	$\mu$	$E_{HOMO}$	$E_{LUMO}$	$\cos Ar$	$\cos Vol$	$L$	Log $K_p$	$\sum q(C)$	$q(N)$	$\mu_e$
Log $P_{o/w}$	1	0.846	0.604	−0.472	0.999	0.853	0.743	0.999	0.956	−0.543	0.995
$\mu$		1	0.935	−0.869	0.867	0.991	0.275	0.866	0.653	−0.332	0.974
$E_{HOMO}$			1	−0.987	0.632	0.931	−0.084	0.418	0.065	0.244	0.521
$E_{LUMO}$				1	−0.503	−0.864	−0.953	−0.271	−0.019	−0.481	−0.384
$\cos Ar$					1	0.871	−0.449	0.968	0.944	−0.515	0.991
$\cos Vol$						1	−0.342	0.719	0.649	0.008	0.796
$L$							1	0.87	0.906	−0.966	0.807
Log $K_p$								1	0.997	−0.713	0.993
$\sum q(C)$									1	−0.766	0.981
$q(N)$										1	−0.841
$\mu_e$											1

have the highest values in PC liposomes, the membrane penetration of these dyes may be driven mainly by hydrophobic effects. Additional confirmation for penetration of amidinobenzanthrones in the membrane hydrophobic region came from the study of energy transfer between anthrylvinyl-labeled phosphatidylcholine (energy donor) and benzanthrone dyes (acceptor) (data are not presented here). The calculated distances between the lipid bilayer midplane and fluorescent probes AM12, AM15 and AM18 were found to be to 0.9 nm, 1.1 nm and 1.3 nm, respectively, indicating that the dyes are located in the region of hydrocarbon chains. Accordingly, the lower extent of membrane partitioning of these dyes in the presence of Chol can be interpreted in terms of Chol-induced rigidification of the membrane hydrophobic region [36,37]. As seen in Table 2, the partition coefficients of AM12, AM15 and AM18 in CL-containing membranes decrease compared to the neat PC liposomes proportionally to CL content: the higher the CL content, the smaller the calculated  $K_p$  value. A reasonable interpretation of the decrease in the observed  $K_p$  comes from the higher-resolution atomic simulation of membranes composed of CL alone and its mixtures with POPC [34]. These studies suggest that CL bilayers are more ordered than PC bilayers, since incorporation of CL into PC bilayers have a significant ordering effect, even at small CL concentrations. Obviously, this ordering effect prevents partitioning of highly hydrophobic aminobenzanthrones into CL-containing membranes. Furthermore, allowing for Chol and CL ability to affect the dipole potential of the PC bilayer [30], one cannot rule out the possibility that benzanthrone partitioning is controlled by the membrane dipole potential. As indicated above,  $\psi_d$  depends on orientation of phosphocholine and ester carbonyl dipoles of phospholipids and molecular dipoles of interfacial water. The conical shape of CL molecule induces a negative curvature strain, so that the bilayer polar region becomes more accessible to water. The resulting changes in the membrane dipole potential may prove essential in the membrane incorporation of both amino- and amidino-benzanthrone derivatives. It is noted that IBH exhibits a completely different behavior compared with ISH and IAH, since the observed partition coefficients in the model membranes composed of PC and its mixtures with CL seem to be identical. Furthermore, the IBH partition coefficient in Chol-containing membranes is rather large in comparison with those

of IAH and IBH. Substantial scattering of the partition coefficients for the aminobenzanthrone dyes are ascribed to considerably lower fluorescence intensities and quantum yields of these dyes in the model membranes (especially in the case of IBH in the CL and Chol-containing membranes) compared with the amidino derivatives. Low fluorescence intensity along with the absence of saturation (for IAH) may be the source of large errors in determination of aminobenzanthrone's partition coefficients, complicating a comparison of the dye membrane affinities. However, the results presented above indicate that amino substitution at the C-3 position of the benzanthrone core substantially decreases affinity of benzanthrone dyes to the model membranes. This observation may prove itself useful for synthesis of new dyes for biomedical application.

#### 4.3. Correlation analysis

To correlate experimentally determined partition coefficients (log  $K_p$ ) with physicochemical properties of the examined compounds, we calculated a series of molecular descriptors tentatively divided into three groups: (i) lipophilicity descriptor (log  $P_{o/w}$ ), (ii) geometrical (steric) descriptors ( $\cos Ar$ ,  $\cos Vol$ , and  $molLen$ ) and (iii) quantum chemical descriptors ( $q(N)$ ,  $\sum q(C)$ ,  $\mu$ ,  $\mu_e$ ,  $E_{HOMO}$ , and  $E_{LUMO}$ ) (Table 3). Next, allowing for the foresaid differences between the amidino- and amino derivatives it seemed reasonable to perform separate correlation analysis for each of these groups. As seen in Tables 4 and 5, in both groups the highest correlation was observed between the experimental partition coefficient log  $K_p$  and calculated lipophilicity descriptor log  $P_{o/w}$ . Lipophilicity, an important molecular parameter widely used in QSPR analysis, characterizes the tendency of a molecule to distribute between water and water-immiscible solvent [38]. This parameter can be expressed by a volume or cavity term accounting for hydrophobic and dispersion forces, and polarity term determined by electrostatic interactions [39,40]. The polar interactions encoded in log  $P_{o/w}$  involve hydrogen-bonds, orientation and induction forces. The values of log  $P_{o/w}$  were found to fall in the range 5.28–7.18, indicating that the examined dyes possess rather high lipophilicity comparable to that of other dyes (for instance, log  $P_{o/w}$  was reported to be ~4 to 6.5 for porphyrins [41] or 1.7–5.6

**Table 5**  
Correlation matrix for physicochemical descriptors of IAH, IBH and ISH.

	Log $P_{o/w}$	$\mu$	$E_{HOMO}$	$E_{LUMO}$	cosAr	cosVol	L	Log $K_p$	$\Sigma q(C)$	$q(N)$	$\mu_e$
Log $P_{o/w}$	1	0.961	0.907	0.979	0.352	0.239	0.536	0.998	0.516	-0.579	-0.823
$\mu$		1	-0.435	-0.632	-0.863	-0.796	-0.954	0.974	-0.782	0.012	0.976
$E_{HOMO}$			1	0.973	-0.075	-0.192	0.13	-0.661	0.112	-0.187	-0.618
$E_{LUMO}$				1	0.158	0.041	0.356	-0.537	0.339	-0.409	-0.784
cosAr					1	0.993	0.978	-0.956	0.979	-0.966	-0.736
cosVol						1	0.948	-0.915	0.947	-0.923	-0.624
L							1	-0.996	0.999	-0.966	-0.870
Log $K_p$								1	-0.993	0.999	0.902
$\Sigma q(C)$									1	-0.997	-0.898
$q(N)$										1	-0.206
$\mu_e$											1

for anthrahydroquinones [42]). Since the benzanthrone part is identical for all of the examined compounds, the differences in lipophilicity are ascribed to functionalities in their structure, viz., amidino (AM12, AM15, and AM18) and amino group (ISH, IAH, and IBH) in the C-3 position, phenyl ring (ISH, IAH, IBH, AM12 and AM18), methyl (AM18 and AM12), ethyl (AM15), methoxy (IAH) and highly hydrophilic hydroxy (ISH) groups.

Correlation analysis points to the importance of geometrical descriptors, such as cosmo area, cosmo volume and molecular length in determining the  $K_p$  value for AM12, AM15 and AM18 (Table 4). On the contrary, correlation between geometrical descriptors of aminobenzanthrones and  $K_p$  is negative, suggesting that hydrophilic properties of these compounds are expressed more strongly than those of amidino derivatives (Table 5). It is noteworthy that not all of the calculated quantum-chemical parameters had an effect on the partition coefficient. Apart from the geometric parameters, the dipole moment of all benzanthrone derivatives showed a marked positive correlation with the partition coefficient. In QSAR/QSPR analyses the dipole moment is the most appropriate quantity to describe polarity of a certain compound [43]. The  $\mu$  values were found to rise in the order ISH–IBH–IAH–AM15–AM12–AM18, indicating an increase in molecular polarity from IAH to AM18. Likewise, very high positive correlation has been found between the experimental partition coefficients and dipole moments of the excited state for both groups of the dyes. It should be noted that the excited-state dipole moments of all benzanthrone derivatives are rather high compared to their ground-state ones, suggesting a substantial redistribution of the  $\pi$ -electron densities in a more polar excited state. Furthermore, significant change in the dipole moment upon excitation indicates that the excited state is a twisted intramolecular charge-transfer (TICT) in nature. Along with dipole moments, charge based descriptors, such as atomic partial charges and their sums, have been widely employed as chemical reactivity indices or as a measure of weak intermolecular interactions [43–46]. Therefore it was interesting to evaluate how partition properties of the dyes under study depend on atomic charges. To this end, we chose the sum of charges on the carbon atoms and the net charge on the nitrogen atom at the C3-position as molecular descriptors. It appeared that the partition coefficient strongly correlates with a sum of charges on the carbon atoms, but the signs of correlation coefficients are opposite for the amidino- and amino derivatives. On the other hand, high correlation between the  $K_p$  value and the net charge on the nitrogen atom was found only for the aminobenzanthrones.

The correlations between the experimentally determined partition coefficients and calculated molecular descriptors confirm complex nature of interactions between the examined fluorescent dyes and model membranes, reflected in Eq. (8). Specifically, a linear dependence between lipophilicity and  $K_p$  allowed us to hypothesize that bilayer partitioning of benzanthrone is largely

**Table 6**  
Fluorescence anisotropy of benzanthrone dyes in different lipid systems.

Dye	PC	PC/CL (5%)	PC/CL (10%)	PC/Chol (30%)
AM12	0.236	0.256	0.265	0.263
AM15	0.197	0.222	0.232	0.215
AM18	0.197	0.229	0.248	0.223
IAH	0.188	0.201	0.198	0.192
IBH	0.189	0.188	0.191	0.203
ISH	0.224	0.224	0.218	0.222

driven by hydrophobic interactions. Furthermore, high correlation coefficient between  $K_p$  and the dipole moment indicates the importance of dipole–dipole interactions for the dye partitioning, especially for the amino derivatives. Additional arguments in favor of this assumption come from the fact that the partition coefficients of the aminobenzanthrones become higher in the presence of cholesterol, which is capable of increasing the dipole moment of lipid bilayer [30].

#### 4.4. Solvent relaxation and fluorescence anisotropy studies

Previously, we tested another series of benzanthrone amino derivatives, to assess their potential, by monitoring the changes in physicochemical properties of model membranes [12]. All of these dyes exhibited red edge excitation shift (REES), which is not surprising in view of benzanthrone's ability to ICT from amine substituent to carbonyl group. The red edge effect is known to originate from the differences in fluorophore–solvent interactions between ground and excited states; such differences are determined by the changes in the dye dipole moment upon excitation and the rate of solvent reorientation around excited state fluorophore [46]. In the steady-state fluorescence measurements REES manifests itself as a shift of emission maximum towards longer wavelengths with increasing excitation wavelength. It has been demonstrated that the REES magnitude increases in a depth-dependent manner: the less the REES, the deeper the probe locates [47]. However, in the present study we failed to detect REES even for IBH, ISH and IAH residing presumably in the polar membrane region. Red edge excitation shift is observed when a polar fluorophore is placed in motionally restricted media, such as very viscous solutions and condensed phases where dipolar relaxation time of solvent shell around a fluorophore is comparable or longer than its fluorescence lifetime [48]. Therefore, the main reason for the absence of REES is most probably associated with the fact that dipolar relaxation time of the dyes under investigation is considerably shorter than fluorescence lifetime.

Finally the fluorescence anisotropy of benzanthrone dyes was measured in different lipid systems. As illustrated in Table 6, only the anisotropy values of AM12, AM15 and AM18 appeared to be sensitive to the changes in membrane composition. Fluorescence

anisotropy of membrane-bound probes is determined by the rate of its rotational diffusion. Since diffusive motions depend on free volume of the dye microenvironment [9], anisotropy values reflect the changes in lipid packing density. The observation that anisotropy is higher in CL- and Chol-containing membranes confirms the above hypothesis that AM12, AM15 and AM18 reside in the hydrophobic membrane region undergoing condensing effects due to Chol and CL.

## 5. Conclusions

The ability of a series of novel benzanthrone derivatives to trace the changes in membrane structural state was evaluated. All dyes were found to display marked affinity for artificial membranes and high sensitivity to physicochemical properties of the lipid bilayer. Fluorimetric determination of partition coefficients showed that the amidino derivatives exhibit stronger membrane partitioning compared with aminobenzanthrones. The QSPR analysis revealed high correlation between experimentally determined partition coefficients and geometrical parameters of the novel dyes, their lipophilicity and dipole moment, indicating multiplicity of factors contributing to the lipid bilayer affinity of these compounds. High environmental sensitivity of amidinobenzanthrone derivatives allowed us to recommend these probes for membrane studies.

## Acknowledgment

This work was supported by the grant from Fundamental Research State Fund (Project no. F.54.4/015) and CIMO Fellowship (OZ). The authors are indebted to referees for valuable remarks.

## Appendix A. Supplementary material

Supplementary data associated with this article can be found in the online version at <http://dx.doi.org/10.1016/j.jlumin.2013.10.015>.

## References

- [1] M. Refat, S. Aqeel, I. Grabchev, *Can. J. Anal. Sci. Spectrosc.* 49 (2004) 258.
- [2] T. Konstantinova, H. Konstantinov, T. Kaneva, A. Spirieva, *Polym. Degrad. Stab.* 62 (1998) 323.
- [3] F. Carlini, C. Paffoni, G. Boffa, *Dyes Pigm.* 3 (1982) 59.
- [4] I. Grabchev, V. Bojinov, I. Moneva, *J. Mol. Struct.* 471 (1998) 19.
- [5] I. Grabchev, V. Bojinov, I. Moneva, *Dyes Pigm.* 48 (2001) 143.
- [6] I. Grabchev, I. Moneva, E. Wolarz, D. Bauman, *Dyes Pigm.* 58 (2003) 1.
- [7] O. Hrolova, N. Kunavin, I. Komlev, M. Tavrizova, *J. Appl. Spectrosc.* 41 (1984) 53.
- [8] E. Kirilova, I. Kalnina, G. Kirilov, I. Meirovics, *J. Fluoresc.* 18 (2008) 645.
- [9] J. Lakowicz, *Principles of Fluorescence Spectroscopy*, third ed., Springer New York, 2006.
- [10] X. Yang, W.-H. Liu, W.-J. Jin, G.-L. Shen, R.-Q. Yu, *Spectrochim. Acta A* 55 (1999) 2719.
- [11] G. Gorbenko, V. Trusova, E. Kirilova, G. Kirilov, I. Kalnina, A. Vasilev, S. Kaloyanova, T. Deligeorgiev, *Chem. Phys. Lett.* 495 (2010) 275.
- [12] V. Trusova, E. Kirilova, I. Kalnina, G. Kirilov, O. Zhytniakivska, P. Fedorov, G. Gorbenko, *J. Fluoresc.* 22 (2012) 953.
- [13] I. Kalnina, R. Bruvere, T. Zvagule, N. Gabruseva, A. Volrate, G. Feldman, I. Klimkane, E. Kirilova, I. Meirovics, *Proc. Latv. Acad. Sci.* 60 (2006) 113.
- [14] I. Kalnina, L. Klimkane, E. Kirilova, M.M. Toma, G. Kizane, I. Meirovics, *J. Fluoresc.* 17 (2007) 619.
- [15] S. Gonta, M. Utinans, G. Kirilov, S. Belyakov, I. Ivanova, M. Fleisher, V. Savenkov, E. Kirilova, *Spectrochim. Acta A* 101 (2013) 325.
- [16] B. Mui, L. Chow, M. Hope, *Methods Enzymol.* 367 (2003) 3.
- [17] G. Bartlett, *J. Biol. Chem.* 234 (1959) 466.
- [18] M. Schmidt, K. Baldrige, J. Boatz., S. Elbert, M. Gordon, J. Jensen, S. Koseki, N. Matsunaga, K. Nguyen, S. Su, T. Windus, M. Dupus, J. Montgomery, *J. Comput. Chem.* 14 (1993) 1347.
- [19] N. Santos, M. Prieto, M. Castanho, *Biochim. Biophys. Acta* 2003 (1612) 123.
- [20] V. Ivkov, G. Berestovsky, *Dynamic Structure of Lipid Bilayer*, Nauka, Moscow, 1981.
- [21] G. Cevc, *Biochim. Biophys. Acta* 1031 (1990) 311.
- [22] J. Tocanne, J. Teissie, *Biochim. Biophys. Acta* 1031 (1990) 111.
- [23] R. Flewelling, W. Hubbel, *Biophys. J.* 49 (1986) 541.
- [24] M. Belaya, *Langmuir* 3 (1987) 648.
- [25] Y. Levine, *Prog. Biophys. Mol. Biol.* 24 (1972) 1.
- [26] A. McLaughlin, P. Cullis, M. Hemminga, D. Hault, G. Radda, G. Ritchie, P. Seeley, R. Richards, *FEBS Lett.* 57 (1975) 213.
- [27] C. Ho, S. Slater, C. Stubbs, *Biochemistry* 34 (1995) 6188.
- [28] M. Straume, B. Litman, *Biochemistry* 26 (1987) 5121.
- [29] R. Demel, B. de Kruijff, *Biochim. Biophys. Acta* 457 (1976) 109.
- [30] T. Starke-Peterkovic, N. Turner, M. Vitha, M. Waller, D. Hibbs, R. Clarke, *Biophys. J.* 90 (2006) 4060.
- [31] M. Pasenkiewicz-Gierula, T. Rog, K. Kitamura, A. Kusumi, *Biophys. J.* 78 (2000) 1376.
- [32] D. Bach, I. Miller, *Biochim. Biophys. Acta* 1368 (1998) 216.
- [33] A. Shibata, K. Ikawa, T. Shimooka, H. Terada, *Biochim. Biophys. Acta* 1192 (1994) 71.
- [34] M. Dahlberg, A. Malimak, *J. Phys. Chem.* 112 (2008) 11655.
- [35] T. Sparrman, P. Westlund, *Phys. Chem. Chem. Phys.* 5 (2003) 2114.
- [36] H. Merkle, W. Subczynski, A. Kusumi, *Biochim. Biophys. Acta* 897 (1987) 238.
- [37] R. Bittman, L. Blau, *Biochemistry* 11 (1972) 4831.
- [38] F. Lombardo, M. Shalaeva, K. Tupper, F. Gao, M. Abraham, *J. Med. Chem.* 43 (2000) 2922.
- [39] G. van Balen, C. Martinet, G. Caron, G. Bouchard, M. Reist, P. Carrupt, R. Fruttero, A. Gasco, B. Testa, *Med. Res. Rev.* 3 (2004) 299.
- [40] C. Giaginis, A. Tsantili-Kakoulidou, *J. Pharm. Sci.* 97 (2008) 2984.
- [41] M. Kepczynski, R. Pandian, K. Smith, B. Ehrenberg, *Photochem. Photobiol.* 76 (2002) 127.
- [42] R. Singh, M. Dasb, K. Raj, S. Khanna, *Skin Pharmacol. Appl. Skin Physiol.* 13 (2000) 165.
- [43] N. Bodor, Z. Gabanyi, C.-K. Wong, *J. Am. Chem. Soc.* 111 (1989) 3783.
- [44] I. Doichinova, R. Natheva, D. Mihailova, *Eur. J. Med. Chem.* 29 (1994) 133.
- [45] G. Klopman, L. Iroff, *Comp. Chem.* 2 (1981) 157.
- [46] W. Galley, R. Purkey, *Proc. Natl. Acad. Sci. USA* 67 (1970) 1116.
- [47] A. Chattopadhyay, S. Mukherjee, *J. Phys. Chem.* 103 (1999) 8180.
- [48] A. Chattopadhyay, S. Mukherjee, *Biochemistry* 32 (1993) 3804.